

# Model calculations of the proximity effect in finite multilayers

C. Ciuhu and A. Lodder

Faculty of Sciences / Natuurkunde en Sterrenkunde, Vrije Universiteit, De Boelelaan 1081,  
1081 HV Amsterdam, The Netherlands

(October 30, 2018)

The proximity-effect theory developed by Takahashi and Tachiki<sup>1</sup> for infinite multilayers is applied to multilayer systems with a finite number of layers in the growth direction. The purpose is to investigate why previous applications to infinite multilayers fail to describe the measured data satisfactorily<sup>2</sup>. Surface superconductivity may appear, depending on the thickness of the covering normal metallic  $N$  layers on both the top and the bottom. The parameters used are characteristic for V/Ag and Nb/Pd systems. The nucleation process is studied as a function of the system parameters.

## I. INTRODUCTION

An alternating sequence of superconductor and normal metal layers (S/N) generates a system whose properties have raised both theoretical and experimental interests. The dirty-limit theory of Takahashi and Tachiki<sup>1</sup> is meant to describe such systems. However, it has some insufficiencies in explaining experimental results such as the dimensional crossover in  $H_{c2,\parallel}(T)$  curves,<sup>2,3</sup> displaying the upper critical field applied parallel to the layers as a function of the temperature. Since up to now exact calculations using this theory were done for infinite periodic systems, we extend the calculations to finite multilayers. A marked difference is found in the proximity effect on the pair amplitude for the upper critical magnetic fields  $H_{c2,\perp}$  and  $H_{c2,\parallel}$ . In trying to cover as many aspects as possible which underlie the physics in such systems, we are hoping to prepare a theoretical explanation of the experimentally observed dimensional crossover in the parallel upper critical field  $H_{c2,\parallel}$  versus temperature, which improves upon the at present available explanation, being a rather artificial *ad hoc* explanation.<sup>2</sup> We apply the theory to real systems such as finite multilayers of V/Ag.

Section II gives a brief survey of the Takahashi-Tachiki theory. In Section III we calculate the spatial distribution of the pair amplitude, showing features of the proximity effect, which are typical for layered systems. Two distinct situations are treated separately, namely one in which the magnetic field applied to the system is perpendicular to the layers and the other one when the field is parallel to the layers. Section IV is devoted to nucleation properties, which form an intriguing particularity of superconductivity when a parallel magnetic field is applied. The manifestation of surface superconductivity and related problems, such as the influence and role played by the boundary conditions, are treated. In Section V we will present a detailed description of the dependence of the proximity effect on the parameters of the system. The results obtained restore confidence in the applied microscopic theory for dirty multilayers.

## II. THE TAKAHASHI-TACHIKI THEORY

In inhomogeneous systems such as S/N multilayers, the superconducting properties are influenced by the proximity of different materials. One can think of non-superconducting materials, or of superconducting materials with a lower  $T_c$ . A finite Cooper pair amplitude is induced in the less- or non-superconducting material. This proximity effect leads to a reduction of the critical temperature  $T_c$  compared to that of a bulk superconductor.

We will apply the description developed by Takahashi and Tachiki, which has been devised to be valid for inhomogeneous superconductors in the dirty limit.<sup>1</sup> We now give a brief summary of the main equations, by that also defining the system parameters to be used.

The theory starts from the Gor'kov equation<sup>4</sup> for the pair potential  $\Delta(\mathbf{r})$

$$\Delta(\mathbf{r}) = V(\mathbf{r})kT \sum_{\omega} \int d^3\mathbf{r}' Q_{\omega}(\mathbf{r}, \mathbf{r}') \Delta(\mathbf{r}'), \quad (1)$$

in which the material parameter  $V(\mathbf{r})$  is the space dependent BCS coupling constant and the integration kernel  $Q_{\omega}$  obeys a Green's function like equation

$$[2|\omega| + L(\nabla)]Q_{\omega}(\mathbf{r}, \mathbf{r}') = 2\pi N(\mathbf{r})\delta(\mathbf{r} - \mathbf{r}'). \quad (2)$$

The differential operator is defined by

$$L(\nabla) = -\hbar D(\mathbf{r})(\nabla - \frac{2ie}{\hbar c} \mathbf{A}(\mathbf{r}))^2. \quad (3)$$

The material parameters  $N(\mathbf{r})$  and  $D(\mathbf{r})$  are the electronic density of states at the Fermi energy and the diffusion coefficient, respectively.  $V(\mathbf{r})$ ,  $N(\mathbf{r})$  and  $D(\mathbf{r})$  are constant in each single layer. At the interfaces de Gennes boundary conditions are imposed,<sup>5</sup> which require the continuity of  $\frac{F(\mathbf{r})}{N(\mathbf{r})}$  and  $D(\mathbf{r})(\nabla - \frac{2ie}{\hbar c} \mathbf{A}(\mathbf{r}))F(\mathbf{r})$ , where the pair amplitude  $F(\mathbf{r})$  is related to the gap function  $\Delta(\mathbf{r})$  through

$$\Delta(\mathbf{r}) = V(\mathbf{r})F(\mathbf{r}). \quad (4)$$

Takahashi and Tachiki provide a way of solving Eqs. (1) and (2) by developing the kernel  $Q_\omega(\mathbf{r}, \mathbf{r}')$  and the pair function  $F(\mathbf{r})$  in terms of a complete set of eigenfunctions of the operator  $L(\nabla)$ . These eigenfunctions are labeled by the parameter  $\lambda$ , and the eigenvalues are  $\epsilon_\lambda$ . They are solution of the eigenvalue problem

$$L(\nabla)\Psi_\lambda = \epsilon_\lambda \Psi_\lambda. \quad (5)$$

The requirement of the existence of a solution for Eq. (1) leads to the equation

$$\det |\delta_{\lambda\lambda'} - 2\pi kT \sum_\omega \frac{1}{2|\omega| + \epsilon_\lambda} V_{\lambda\lambda'}| = 0. \quad (6)$$

For finite multilayers covered by infinite N layers, the boundary conditions at infinity, imposed in determining the eigenfunctions  $\Psi_\lambda(x, y, z)$  of the differential operator  $L(\nabla)$ , are such that  $\Psi_\lambda(z \rightarrow \pm\infty) = 0$ , which is in line with  $F(z \rightarrow \pm\infty) = 0$ . As usual for these type of layered systems, the growth direction coincides with the  $z$  direction. For finite multilayers in vacuum, we apply de Gennes boundary conditions, since they insure that there is no current flow through the interface between the multilayer and the vacuum. These boundary conditions read  $\frac{\partial \Psi_\lambda(x, y, z)}{\partial z} = 0$  at the interface with the vacuum. In the absence of a magnetic field, the solution of Eq. (6) giving the largest value for the critical temperature is the physical one. In the presence of a field, solving this equation allows us to derive the  $H_{c2}(T)$  curves. The temperature at which  $H_{c2} \rightarrow 0$  is  $T_c$ .

### III. THE PERPENDICULAR AND PARALLEL UPPER CRITICAL MAGNETIC FIELDS

We consider a multilayer system such as the one depicted in FIG. 1. A certain number of finite-thickness S/N layers are covered by infinitely thick external N-layers in the growth direction  $z$ . We will vary the number of internal layers, and show results for systems with 1, 5, 9, and 69 internal layers respectively. A magnetic field of magnitude 1 kGauss is applied in the growth direction, so perpendicular to the layers. The computation and analysis of the pair function will lead us to some interesting conclusions related to the microscopic aspects of the proximity effect.

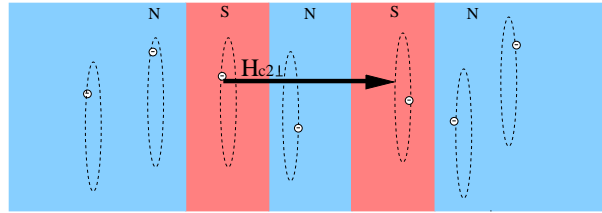


FIG. 1. The movement of the electrons in the system, when a perpendicular magnetic field is applied.

For a perpendicular orientation of the field we can choose  $\mathbf{A}(\mathbf{r}) = (0, Hx, 0)$ . By that, applying the method of separation of variables, we can write the solution  $\Psi_\lambda$  of Eq. (5) as

$$\Psi_\lambda = w_{a_x}(x)e^{ik_y y}\Phi_\lambda(z) \quad (7)$$

The solutions in the  $x$  direction are parabolic cylinder functions, which for the present case are equivalent to one-dimensional harmonic oscillator functions. The system is infinite and uniform in the  $x$  and  $y$  directions, so that the ground state has  $a_x = -\frac{1}{2}$  and arbitrary  $k_y$ . With  $\Psi_\lambda$  given by Eq. (7), Eq. (5) reduces to

$$-\frac{d^2}{dz^2}\Phi_\lambda(z) = k_\lambda^2(z)\Phi_\lambda(z), \quad (8)$$

with

$$k_\lambda^2(z) = \frac{\epsilon_\lambda}{\hbar D(z)} - \frac{1}{\xi^2}, \quad (9)$$

in which the magnetic coherence length  $\xi = \sqrt{\frac{\hbar c}{2eH}}$ .

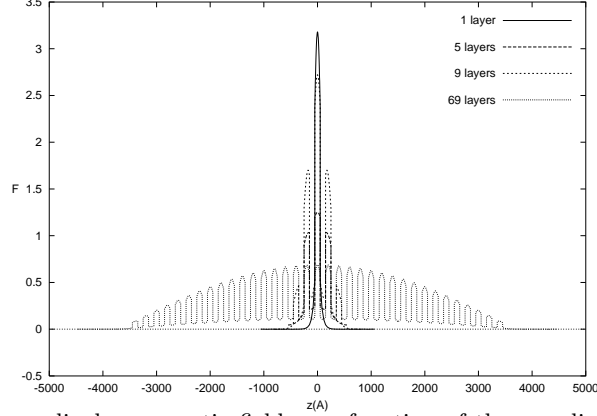


FIG. 2. The pair function in perpendicular magnetic field as a function of the coordinate  $z$  in the growth direction. The thickness of both N and S layers are  $d_S = d_N = 100\text{\AA}$ . The magnetic field applied is  $H_\perp = 1\text{ kGauss}$ .

In FIG. 2 the pair function is shown for four systems with a different number of internal layers. The system parameters used are specific for V/Ag multilayers<sup>6-9</sup>. Two features of the proximity effect come out clearly. One is that the proximity of the S and N layers leads to the oscillating behavior, in which the minima correspond to the N layers, while the maxima occur within the S layers. The other one is an overall proximity effect due to the infinite exterior  $N$ -layers. The 69-layers result can be considered as to stand for the limit of a large number of layers. The influence of the outer layers is not noticed any more in the middle of the system, the behavior here becoming similar to that of an infinite periodic system, described by Koperdraad et al.<sup>2</sup>

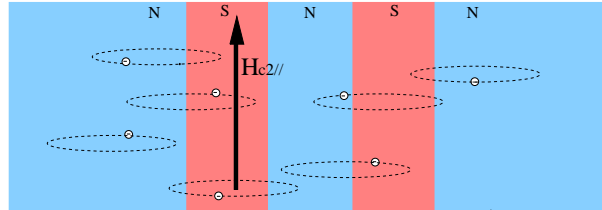


FIG. 3. The movement of the electrons in the system, when a parallel magnetic field is applied.

Turning to the parallel field case, we first show in FIG. 3 in an intuitive way how the electrons move. This leads to a movement of the Cooper pairs in which they would extend naturally in the normal layers. But as they are forbidden there, the concentration of Cooper pairs in the superconducting layers will be pushed up. As in the perpendicular field case, the outer  $N$  layers extend to infinity.

To compute the pair functions, we go back to Eq. (5). A parallel magnetic field lies in the  $xy$ -plane, and we can choose the vector potential  $\mathbf{A}(\mathbf{r})$  as  $(Hz, 0, 0)$ . Separation of the variables leads to the form

$$\Psi_\lambda = e^{ik_x x} e^{ik_y y} w_\lambda(z) \quad (10)$$

for  $\Psi_\lambda$ , and the equation for  $w_\lambda$  can be written as

$$\left(-\frac{d^2}{dz^2} + \frac{(z - z_0)^2}{\xi^4} + k_y^2\right)w_\lambda(z) = \frac{\epsilon_\lambda}{\hbar D(z)}w_\lambda(z). \quad (11)$$

The point  $z_0 \equiv \xi^2 k_x$  is called the nucleation point. For the results to be presented in this section the nucleation point is chosen in the middle of the system, so  $z_0 = 0$ . In the following section it will become clear, that this symmetry-inspired choice is not the only possibility, particularly if the covering  $N$  layers are no longer infinitely thick and the system becomes really finite in the growth direction.

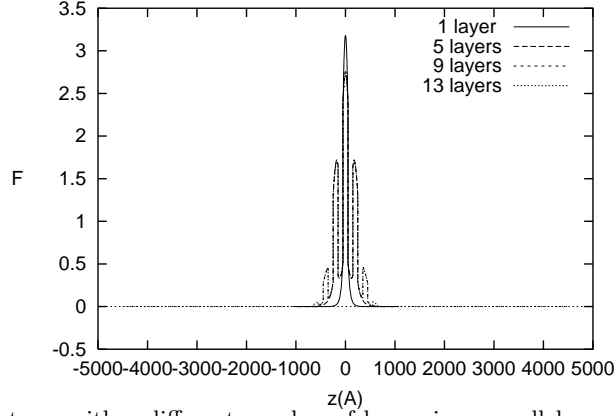


FIG. 4. The pair function for systems with a different number of layers in a parallel magnetic field, for the layer thickness  $d_S = d_N = 100\text{\AA}$ . The applied magnetic field is  $H_{\parallel} = 7\text{ kGauss}$ .

In FIG. 4 we show the pair functions of the systems containing 1, 5, 9, and 13 internal layers. The markedly different behaviour compared to what was found for the perpendicular field case is certainly due to the anisotropy of the system. For each system considered, the pair function drops to zero, except for a few layers, centered around the nucleation point  $z_0$ . Apparently now the proximity effect, here being equivalent to the spreading of the pair amplitude, is much weaker than for  $H_{c2,\perp}$ . The result shown is obtained for a magnetic field of 7 kGauss, which is somewhat larger than the field used in the perpendicular field case. In the latter case the features of the pair distribution are insensitive to the magnitude of the magnetic field. But it appears that in the parallel field case, the higher the field is, the more the pair function is concentrated at the center. So one expects not much difference in the  $H_{c2,\parallel}(T)$  curves for lower temperatures. This is illustrated nicely by FIG. 5, in which these curves are shown for the monolayer and 5-layers systems. The  $H_{c2,\perp}(T)$  curves are shown as well. The  $H_{c2,\parallel}(T)$  curves indeed coincide for higher parallel magnetic fields, irrespective to the number of internal layers considered, but they are clearly different for a small parallel magnetic field. This is related to the fact, that for small magnetic fields, the pair function is spread over the multilayer, in a similar way as it is for the perpendicular magnetic field.

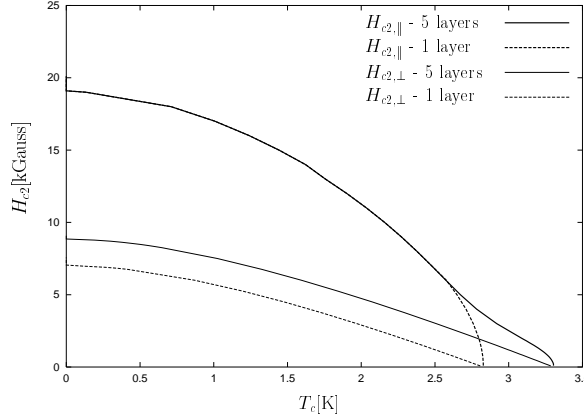


FIG. 5.  $H_{c2,\parallel}(T)$  and  $H_{c2,\perp}(T)$  curves.

The fact that the parallel upper critical field is larger than the perpendicular field is a consequence of the difference in the distribution of the pair amplitude for the two field directions. In the parallel field case, the pairs are concentrated in the S layers. That is why for this direction a larger magnetic field is needed to destroy the superconductivity. A similar argument explains the fact, that  $H_{c2,\perp}$  for five layers is larger than for one layer. Since for  $H_{c2,\perp}$  the pair amplitude is spread over the layers, a 5-layers system is a better superconductor than a one-layer system for all temperatures. Consequently, a one-layer system is expected to have a lower  $T_c$  than a 5-layers system. This is shown clearly by the  $H_{c2,\perp}(T)$  curves, and that is why the parallel curves converge to the perpendicular ones in the zero-field limit.

Now we turn to really finite systems, for which the covering  $N$  layers are finite as well.

#### IV. SEARCH FOR THE NUCLEATION POINT

Measurements of the parallel upper critical magnetic field  $H_{c2,\parallel}$  for multilayer systems such as V/Ag<sup>6-9</sup> show interesting features, such as the dimensional crossover in  $H_{c2,\parallel}(T)$  curves. A generic  $H_{c2,\parallel}(T)$  curve is divided in three regions. Near  $T_c$ , there is an average 3D behavior, corresponding to a linear dependence of the critical magnetic field on the temperature. At a lower temperature, at which the magnetic coherence length becomes of the order of the layer thickness, this behavior is replaced with a square-root-like dependence of  $H_{c2,\parallel}$  on  $T$ , corresponding to a 2D domain. A second dimensional crossover is only present in S/S' systems, which comes from a difference in diffusion constants for the two superconductors, and to which we do not pay further attention.<sup>10,11</sup>

Up to now, the occurrence of the dimensional crossover has not been described satisfactorily. The calculated crossover temperature appears to lie much higher than the measured one.<sup>2</sup> But the results obtained so far only apply for infinite periodic multilayers. Such model systems have translational symmetry in the growth direction, so that surface effects are excluded. It was Aarts who suggested to investigate finite size effects, which always may show up in the finite samples used in experiments.<sup>10</sup>

An extension of the applications of the theory to finite systems is not a trivial one. The reason is, that in calculating the parallel upper critical magnetic field one has to consider the position of the nucleation point  $z_0$ . In infinite periodic systems, nucleation always occurs in the middle of a layer, due to the periodical symmetry of the system. Each center of a layer is a mirror-symmetry center. One only has to figure out which layer of the two types of layers will correspond to the optimal nucleation. In practice this has led to a distinction of two possible solutions, a first solution corresponding to nucleation in the S layers, and a second solution describing nucleation in the N layers.<sup>2</sup>

For finite multilayers the symmetry is largely reduced. Due to mirror-symmetry with respect to the center of the system, one would be inclined to implement the choice of the nucleation point in the center only, as we did in the previous section. But finite systems are known to exhibit surface superconductivity as well. This means that one has to search for the precise location of the nucleation point. If it would turn out to lie close to the surface, it would lie at a point devoid of any symmetry. While surface superconductivity is well investigated in finite homogeneous superconductors, as far as the authors know, such a search has never been done for inhomogeneous layered systems. This is the subject of the present section.

In looking for the correct solution of Eq. (5) it is important to make use of the fact, that the eigenfunctions (10) corresponding to different nucleation points are orthogonal, since they have different wave-numbers  $k_x$ . Due to this, they provide zero-matrix elements in the matrix  $V_{\lambda\lambda'}$ . The determinant (6) will be split in an infinite number of blocks, each block corresponding to a certain nucleation point  $z_0 = \xi^2 k_x$ .

$$\det |\delta_{\lambda\lambda'} - 2\pi kT \sum_{\omega} \frac{1}{2|\omega| + \epsilon_{\lambda}} V_{\lambda\lambda'}| = \prod_{z_0} \det |\delta_{\lambda,z_0;\lambda',z_0} - 2\pi kT \sum_{\omega} \frac{1}{2|\omega| + \epsilon_{\lambda,z_0}} V_{\lambda,z_0;\lambda',z_0}| = 0. \quad (12)$$

In the determinant equation (12), we are interested to solve for that block

$$\det |\delta_{\lambda,z_0;\lambda',z_0} - 2\pi kT \sum_{\omega} \frac{1}{2|\omega| + \epsilon_{\lambda,z_0}} V_{\lambda,z_0;\lambda',z_0}| = 0, \quad (13)$$

which has the highest  $T_c$  as solution for the critical temperature. This will be the physical solution.

Results for an 11-layers system, obtained according to this scheme are shown in FIG. 6. The critical temperature  $T_c$  is plotted as a function of the position of the nucleation point. The system parameters used apply for a V(100Å)/Ag(100Å) system, having a  $H_{c2,\parallel}(0)$  of about 11 kGauss. The specific set of parameters is given in the literature.<sup>6-9</sup>

For a small magnetic field, for 1 and 2 kGauss, the superconductivity occurs in the middle of the multilayer, as the highest  $T_c$  is found for the nucleation point right in the center of the system. For such a small field the size of the system is of the same order of magnitude as  $\xi = \sqrt{\frac{\hbar c}{2eH}}$ , which quantity gives the scaling of the order parameter. For 1 kGauss  $\xi = 574$  Å, which is relatively large compared to the layer thickness. Microscopically, at low parallel magnetic field the pair amplitude is spread over the entire system and looks the same for any choice of the nucleation point  $z_0$ . One could say as well, that for such small fields the entire system is just a surface. At higher parallel magnetic fields, the pairs are confined in about one layer around the position of  $z_0$ . This makes that for higher fields a real difference can be expected for two different  $z_0$  choices. For  $H \geq 3$  kGauss, the nucleation point shifts from the center of the system towards the surface of the sample. For high fields one clearly sees, that superconductivity is found at the surface of the system only.

The shift of the nucleation point towards the surface with increasing magnetic field illustrates the scale of the surface nucleation, which is given by the magnetic coherence length. For a bulk superconductor, if the magnetic field is applied parallel to the interface with the vacuum, the pair function is localized around  $z_0$  nearby the surface<sup>12</sup>

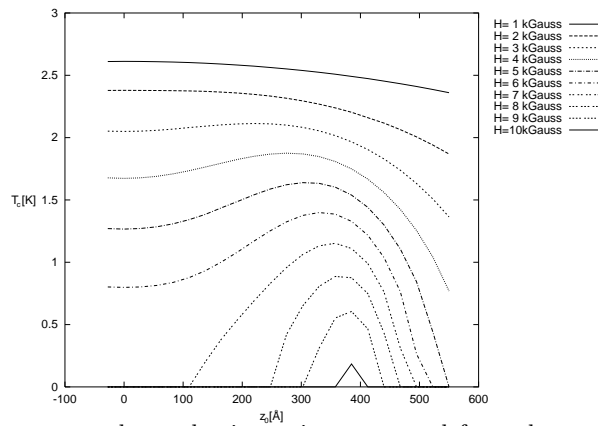


FIG. 6. The critical temperature versus the nucleation point, measured from the center of the layer. The magnetic field varies from 1 to 10 kGauss. Due to the symmetry of the multilayer, we only show one half of the system.

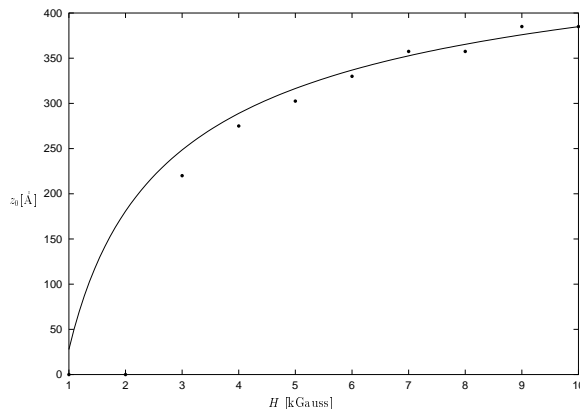


FIG. 7. The points in which the nucleation occurs for different magnetic fields (with dots) fitted in terms of the magnetic coherence length  $\xi$  (continuous line).

$$F \cong \exp\left[-\frac{1}{2}\left(\frac{z - z_0}{\xi}\right)^2\right], \quad (14)$$

in which  $z$  is now measured from the surface, situated at  $z = 0$ . The expression (14) is a gaussian trial function which shows that the pair function is localized around the nucleation point  $z_0$ . A detailed calculation which is based on the exact Weber-function solution shows that  $z_0 \sim \xi$  and the optimal value is  $z_0 = 0.59 \xi$ .

For our multilayer system, the dots in FIG. 7 show the nucleation point as a function of the magnetic field, which can be converted in a dependence on the magnetic coherence length. Measuring  $z_0$  from the surface we find  $z_0 = C\xi$ , where  $C = 0.91$ , which is represented in FIG. 7 by the continuous line. It is not too surprising that this constant for the layered system is larger than the value of 0.59 for a bulk superconductor. The surface phenomena in the present systems will be shifted inward due to the covering  $N$  layer.

The results presented up to now in this section apply to a multilayer system whose outer  $N$  layers have a thickness of  $100\text{\AA}$ , which is equal to the thickness of the  $S$  and  $N$  internal layers. As we were looking at the influence of the boundary on the superconductivity, we studied also systems in which the thickness of the outer  $N$  layers is larger. Keeping all other parameters constant, we only extend the thickness of the exterior layers to  $d_N^{\text{outer}} = 350\text{\AA}$ , such that it becomes larger than the magnetic coherence length  $\xi$ . The corresponding plot of  $T_c$  versus  $z_0$  is given in FIG. 8 for seven magnitudes of the magnetic field. Clearly, up to 5 kGauss the nucleation occurs in the middle of the system. No surface superconductivity does appear anymore since the normal outer layer is thick enough to “screen” it. For larger fields some surface superconductivity shows up again.

In conclusion, in spite of the complexity of the layered systems, relations found between the nucleation and the scaling length  $\xi$  of the superconductivity compare well with established results for homogeneous superconductors. This can be regarded as a support for the validity of the theory of Takahashi and Tachiki, which is devised to describe arbitrary inhomogeneous systems.

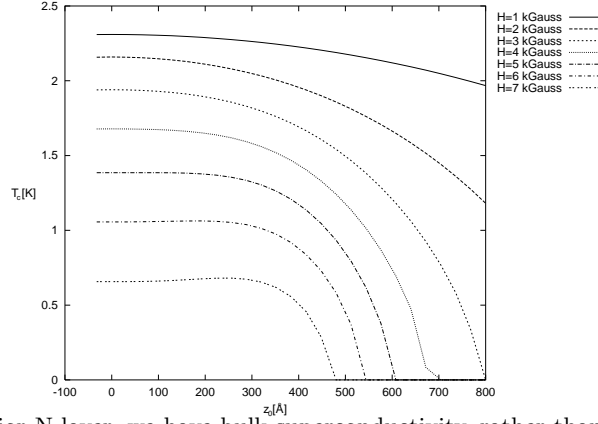


FIG. 8. For a thick exterior N layer, we have bulk superconductivity, rather than surface superconductivity.

## V. THE INFLUENCE OF THE PARAMETERS ON THE PROXIMITY EFFECT

Up to now we have shown properties of finite multilayer systems by varying the applied magnetic field only. In order to prepare a solution to the as yet unsolved problem related to the position of the dimensional crossover in the  $H_{c2,\parallel}(T)$  curves, we need to study the way in which nucleation occurs by varying system parameters as well. In addition to the system parameters mentioned already, such as the diffusion constant for S and N layers and the density of states (DOS) of the S layer, we will consider the resistivity of the interfaces.<sup>13,14</sup> Although we start from parameters which are specific to V/Ag, by varying some of them the set we are using might not characterise this system anymore. On the other hand, we are studying general properties of S/N systems, which means that we have to look not only to a particular system, but to a large class of S/N multilayers.

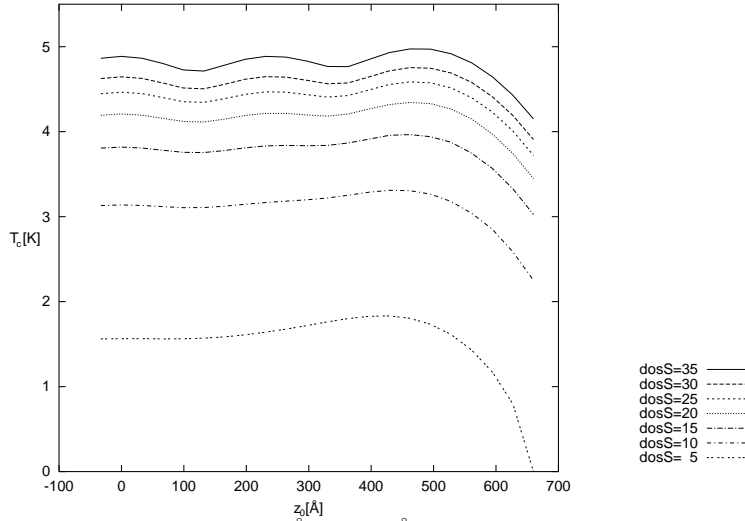


FIG. 9. The nucleation curves for a 11-layers S(120Å)/N(120Å) system, with increasing the S layer DOS.  $H=6$  kGauss and  $D_N = 5 \text{ cm}^2/\text{s}$ .

First we vary the S layer DOS in a S(120Å)/N(120Å) 11-layers system. This is a parameter which measures the density of electrons at the Fermi level. The higher it is, the more Cooper pairs can be formed, so the material is a better superconductor. While varying the S layer DOS, the other parameters keep the same values used before. In FIG. 9 we show the nucleation curves for an increasing DOS of the superconducting layer. The quantity  $\text{dosS}$  gives the ratio of the S layer DOS with respect to the N layer DOS, which covers a large range of DOS values, because in the equations only this ratio contributes. Since the system is symmetric with respect to the center of the multilayer, we only show half of it. First, we notice an increase of the multilayer critical temperature with increase of the S layer DOS, which is a consistent result. Secondly, with the increase of the S layer DOS, we notice a smooth transition from a regime which is dominated by the surface superconductivity, at lower  $\text{dosS}$  values, to a regime in which a modulation develops following the structure of the multilayer. Besides, surface superconductivity is still present by

a slight bump close to the surface. This bump cannot be present in infinite multilayers, having no surface. This is illustrated in FIG. 10, in which the  $\text{dosS} = 25$  result for the finite system, represented by the solid line, is compared to the periodic result for an infinite multilayer. The modulations are such, that the maxima are located at the centers of the superconducting layers. Apparently, for high  $\text{dosS}$  values the proximity effect is not strong enough anymore to smear out the high pair amplitude inside the S layers. This can be understood from the fact that at high  $\text{dosS}$ , the S/N interfaces behave like S/Vacuum interfaces, so that the coupling between the S-layers is very small.

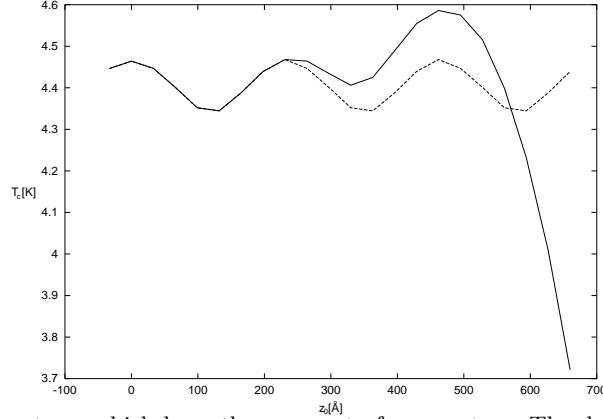


FIG. 10. Nucleation curves for systems which have the same set of parameters. The dashed line corresponds to the infinite periodical multilayer, while the continuous one to a finite 11 layer system.

Now we want to see how the behaviour displayed in FIG. 9 is modified by varying the diffusion constant  $D_N$  of the N layer and by looking at different magnitudes of the magnetic field. We concentrate on two representative curves, namely for  $\text{dosS} = 5$  and 25. Results are shown in FIG. 11.

In FIG. 11(a) we show the evolution of the nucleation curve for  $\text{dosS} = 5$  with increasing diffusion coefficient  $D_N$ , at a lower magnetic field ( $H=2$  kGauss). Even the bump in the  $\text{dosS} = 5$  curve of FIG. 9 has disappeared, because for such a weak field  $\xi$  is large, and there is no surface superconductivity. For larger  $D_N$  values some surface superconductivity shows up again. This is because, in addition to the magnetic coherence length, from now on to be denoted by  $\xi_{mag}$ , the BCS coherence length comes into play. For dirty alloys this quantity is defined as  $\xi_{BCS} = \sqrt{\frac{\hbar D}{2\pi k T}}$ ,<sup>5</sup> and for  $D_N = 20$  cm<sup>2</sup>/s and  $T = 2$  K it is equal to 348 Å. This implies a good coupling between the superconducting layers, by which the entire multilayer develops properties pointing in the direction of a homogeneous superconductor. Because  $\xi_{mag} = 406$  Å, for such a system surface superconductivity could develop at  $0.59 \times 406 = 239$  Å from the surface. The weak maximum in the  $D_N = 20$  curve in FIG. 11(a) lies somewhat more inward.

In FIG. 11(b) the magnetic field has a higher value,  $H=5$  kGauss, which lies close to the value used in FIG. 9. Again  $\text{dosS} = 5$ , and the curve for  $D_N = 6$  is similar to the  $\text{dosS} = 5$  curve of FIG. 9. The effect of increasing  $D_N$  is much more pronounced than for the weaker field, and the maxima of the curves lie at a distance of about  $0.91\xi_{mag} = 371$  Å from the surface. For large  $D_N$  values surface superconductivity is dominantly present.

FIG. 11(c) shows the modifications to the  $\text{dosS} = 25$  curve of FIG. 9. We restricted the calculation to a 7-layer system, by which one oscillation has dropped out. The magnetic field is  $H = 5$  kGauss, slightly weaker than the field used in FIG. 9. The modulation disappears with increasing diffusion coefficient, because a higher  $D_N$  facilitates the coupling between the S-layers.

All three panels of FIG. 11 show a decrease of  $T_c$  with an increasing diffusion coefficient. This can be understood globally in terms of superconducting bulk properties. For a bulk superconductor the only eigenvalue that contributes in the determinant (6) is the ground state eigenvalue, which is proportional to the diffusion constant and the magnetic field, and inversely proportional to the magnetic flux quantum  $\phi_0 = \frac{\hbar c}{2e}$ ,<sup>1,12,15</sup>

$$\epsilon_G = \frac{2\pi\hbar DH}{\phi_0}. \quad (15)$$

Following de Gennes we write  $\epsilon_G$  in Eq. (6) explicitly in terms of the so-called universal function  $\text{Un}(x)$  as<sup>12</sup>

$$\epsilon_G = kT_c(0)\text{Un}\left(\frac{T_c(H)}{T_c(0)}\right), \quad (16)$$

while  $\text{Un}(x)$  is monotonically increasing with decreasing  $x$ . This implies a decrease of  $T_c(H)$  with increasing  $\epsilon_G$ , and therefore, according to Eq. (15), with increasing  $D$ . Also, for a larger magnetic field the effect will be stronger. For



the layered systems an average value of  $D_S$  and  $D_N$  has to be used, but this average increases with increasing  $D_N$ . A decrease of  $T_c$  with increasing  $D_N$  is seen indeed, and also the effect is stronger for a larger field.

The scaling change due to the variation of  $\xi_{mag}$  through its dependence on  $H$  is shown in FIG. 12. The  $H = 6$  kGauss curve reproduces the  $\text{dosS} = 25$  curve of FIG. 9. The nucleation curves show a smooth transition from curves which exhibit only surface superconductivity, to curves in which a modulation over the S and N layers is present. This transition happens when  $H \approx 5$  kGauss and  $\xi_{mag} \approx 257$  Å. This value is comparable with the periodicity of the multilayer,  $d_N + d_S = 240$  Å. In other words, when  $\xi_{mag}$  becomes as small as the periodicity of the multilayer, the nucleation exhibits the modulation corresponding to the geometrical structure of the multilayer. The maxima are located in the S layers and a preference is shown for the superconductivity to nucleate there. Comparing with Fig. 9, in which this modulation appears when the coupling between the S-layers becomes weak at high  $\text{dosS}$ , here this feature of the nucleation curves can again be understood by the fact that the S-layer coupling decreases with the decrease of the coherence length at high magnetic fields.

Finally we vary the boundary resistivity  $\rho_B$  at the interfaces, expressed in units  $\mu\Omega\text{cm}^2$ . Since we have in view interfaces, we restrict our calculations to just a thin superconductor film, covered by a normal metal. We vary  $\rho_B$  around experimental data,<sup>16</sup> which are specific to Nb/Pd systems. We did calculations for a thin film of Nb(600Å) covered by Pd(100Å) at an intermediate magnetic field, which for Nb/Pd is about 12.5 kGauss. The nucleation curves are shown in FIG. 13. We notice that with increasing boundary resistivity  $\rho_B$ , which means that the S/N interfaces become less transparent to the electrons, the critical temperature increases. This can be understood as follows. The interface resistivity makes the spreading of the electrons (Cooper pairs) over the different layers more difficult, which effectively leads to an enhancement of the pair amplitude in the superconducting layers. This weaker proximity effect results in a higher  $T_c$  of the system. This effect is similar to what was discussed in Sec. III regarding  $H_{c2,\parallel}$ , which systematically turned out to be larger than  $H_{c2,\perp}$ .

## VI. CONCLUSIONS

The theory of Takahashi and Tachiki, applied so far either to a bilayer<sup>17</sup> or to infinite multilayers,<sup>1,2</sup> has been applied to describe superconducting properties of finite multilayers. We have calculated the spatial dependent pair amplitude for two magnetic field directions, parallel and perpendicular to the layers. These properties, including the upper critical field curves, have been studied as a function of the number of layers.

The nucleation problem, which appears when one studies systems to which a parallel magnetic field is applied, is illustrated on model systems such as V/Ag multilayers and Nb/Pd thin films for a large range of parameters. Moreover, we compare the results obtained for finite systems to what is found for infinite periodic multilayers. Since we take into account the boundaries, typical for a finite sample, we get surface superconductivity.

Varying the parameters we see how they influence the proximity effect and the scaling of the sample and layer thicknesses to the magnetic and BCS coherence lengths. The superconductivity occurs differently for different choices of the parameters. If we define the dimensional crossover as being the temperature where the modulation over the geometrical structure of the multilayer appears in the nucleation curves, then we must expect a shift of the dimensional crossover in the  $H_{c2,\parallel}(T_c)$  curves under a change of the parameters.

The results we get are meant to prepare an improvement upon the previous approaches in explaining the experimental results.<sup>2</sup> In addition, the results obtained contribute to new confidence in the Takahashi-Tachiki theory. This comes from the observation, that our results about surface superconductivity in finite multilayers, being typically anisotropic systems, can be understood as a generalization of what is known about the phenomenon in isotropic homogeneous superconductors.

## ACKNOWLEDGEMENT

One of the authors (CC) would like to thank Dr. R.T.W. Koopdraad for useful discussions.

---

<sup>1</sup> S. Takahashi and M. Tachiki, Phys. Rev. B **33**, 4620 (1986) and B **34**, 3162 (1986).

<sup>2</sup> R.T.W. Koperdraad and A. Lodder, Phys. Rev. B **51**, 9026 (1995).

- <sup>3</sup> R.T.W. Koperdraad, *The proximity effect in superconducting metallic multilayers* Vrije Universiteit, (1995). Available on request.
- <sup>4</sup> L.P. Gor'kov, Soviet Phys. JETP **10**, 998 (1960).
- <sup>5</sup> P.G. de Gennes, Rev. Mod. Phys. **36**, 225 (1964).
- <sup>6</sup> K. Kanoda, H. Mazaki, T. Yamada, N. Hosoi, T. Shinjo, Phys. Rev. B **33**, 3 (1986).
- <sup>7</sup> K. Kanoda, H. Mazaki, T. Yamada, N. Hosoi, T. Shinjo, Phys. Rev. B **35**, 1 (1987).
- <sup>8</sup> K. Kanoda, H. Mazaki, N. Hosoi, T. Shinjo, Phys. Rev. B **35**, 13 (1987).
- <sup>9</sup> K. Kanoda, H. Mazaki, N. Hosoi, T. Shinjo, Phys. Rev. B **35**, 16 (1987).
- <sup>10</sup> J. Aarts, Phys. Rev. B **56**, 8432 (1997).
- <sup>11</sup> W. Maj and J. Aarts, Phys. Rev. B **44**, 14 (1998).
- <sup>12</sup> P.G. de Gennes *Superconductivity of metals and alloys*, W.A. Benjamin, New York, 1966.
- <sup>13</sup> M.Y. Kupriyanov and V.F. Lukichev, Sov. Phys. JETP **67**, 1163 (1988).
- <sup>14</sup> R.T.W. Koperdraad and A. Lodder, Phys. Rev. B **54**, 515 (1996).
- <sup>15</sup> A. Lodder and R.T.W. Koperdraad, PHYSICA C **212**, 81 (1993).
- <sup>16</sup> S. Kaneko, U. Hiller, J.M. Slaughter, Charles M. Falco, C. Coccorese and L. Maritato, Phys. Rev. B **58**, 13 (1998).
- <sup>17</sup> R.T.W. Koperdraad and A. Lodder, PHYSICA C **268**, 216 (1996).

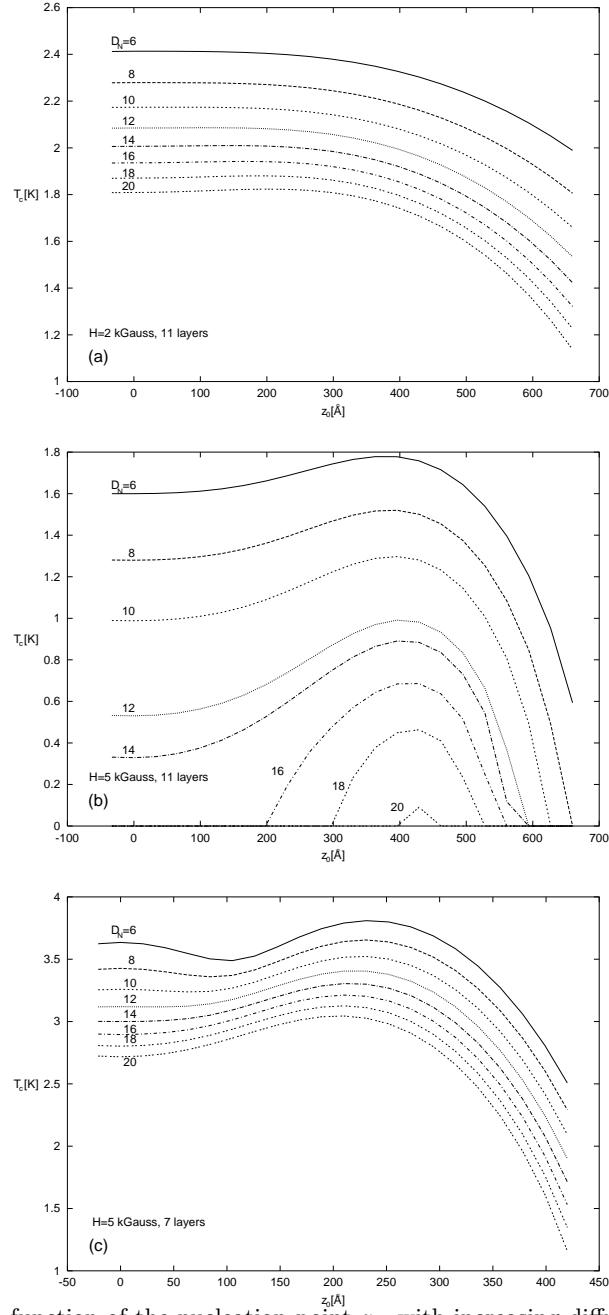


FIG. 11. The temperature as a function of the nucleation point  $z_0$ , with increasing diffusion coefficient of the normal metal  $D_N$ . (a) at  $H=2$  kGauss,  $\frac{\text{SlayerDOS}}{\text{NlayerDOS}} = 5$ ; (b)  $H=5$  kGauss,  $\frac{\text{SlayerDOS}}{\text{NlayerDOS}} = 5$ ; (c)  $H=5$  kGauss,  $\frac{\text{SlayerDOS}}{\text{NlayerDOS}} = 25$ .

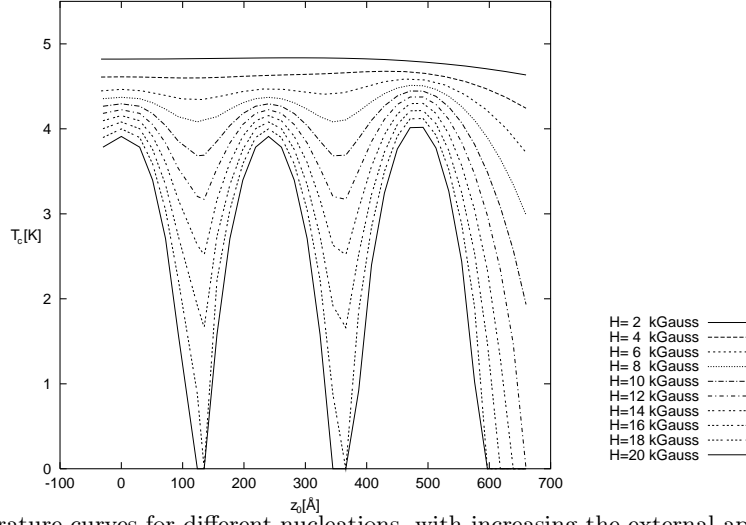


FIG. 12. The temperature curves for different nucleations, with increasing the external applied magnetic field  $H$ .

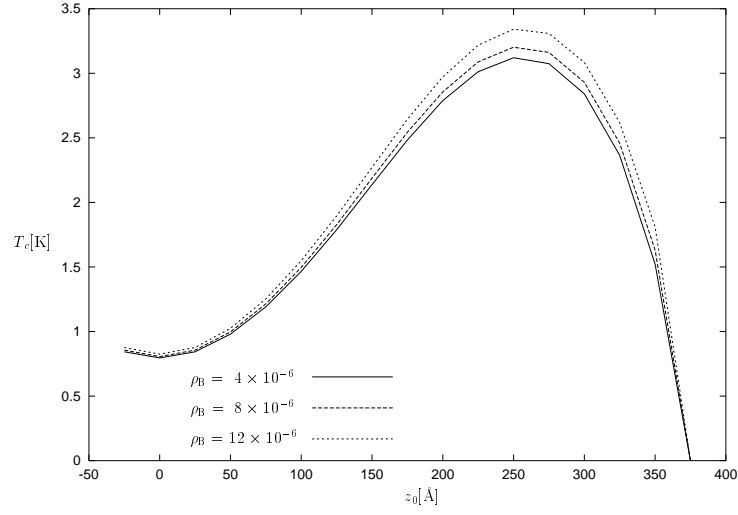


FIG. 13. The nucleation curves for different nucleations, with increasing boundary resistivity  $\rho_B (\mu\Omega\text{cm}^2)$ . The system is a thin film of Nb covered with Pd. The magnetic field applied is  $H=12.5$  kGauss.